Coexistence of Microhemorrhages and Acute Spontaneous Brain Hemorrhage: Correlation with Signs of Microangiopathy and Clinical Data[1]

Montserrat Alemany, MD, PhD
Anna Stenborg, MD
Andreas Terent, MD, PhD
Pirkko Sonninen, MD
Raili Raininko, MD, PhD

Purpose: To evaluate prospectively with magnetic resonance (MR) imaging the coexistence of microhemorrhages (MHs) in white patients with acute spontaneous intraparenchymal hemorrhage (IPH) and acute ischemic stroke and to study the association with imaging findings of microangiopathy and various clinical data.

Materials and Methods: Before examinations, informed consents were signed by either the patient or a relative. The study was carried out with the approval of the local ethics committee. MR imaging was performed in 90 patients with acute stroke: 45 with acute spontaneous IPHs (24 men and 21 women; median age, 65 and 68 years, respectively) and 45 age-matched control subjects without intracranial hemorrhages (26 men and 19 women; median age for both, 67 years), as determined at computed tomography. MR imaging included transverse T1- and T2-weighted spin-echo, transverse fluid-attenuated inversion recovery, transverse and coronal T2*-weighted gradient-echo, and, in 50 patients, diffusion-weighted sequences. Presence of MHs and signs of microangiopathy, such as T2 hyperintensities or lacunae, were recorded in the white and deep gray matter. The relationships between MH and IPH and between MH and T2 hyperintensities were analyzed by means of regression analysis. Different clinical features, such as arterial hypertension or diabetes, were registered and correlated with the image findings by means of regression analysis.

Results: MHs were found in 64% of patients with IPH (29 of 45) and 18% of control subjects (eight of 45). A statistically significant relationship between MH and IPH was determined ($P < .001$). Among the 29 patients with IPH and MH, 24 (83%) had T2 hyperintensities and 13 (45%) had lacunae; among the 16 patients without MH, seven (44%) had T2 hyperintensities and three (19%) had lacunae. A relationship between MH and occurrence and extent of T2 hyperintensities was also identified ($P < .001$). There was no clear relationship with the clinical data studied.

Conclusion: The results support a correlation between the presence of imaging signs of cerebral microangiopathy, clinically silent MHs, and acute IPHs.

[1] From the Departments of Radiology (M.A., R.R.) and Internal Medicine (A.S., A.T.), Uppsala Hospital, Uppsala, Sweden; and the Department of Radiology, Turku University Hospital, Turku, Finland (P.S.). From the 2002 RSNA Annual Meeting. Received March 26, 2004; revision requested June 4; final revision received February 10, 2005; accepted February 22. Supported by grants from the Swedish Medical Research Council, the Stroke Foundation, and the Selander Foundation.

The presence of incidental foci of signal intensity loss has been detected with susceptibility-weighted magnetic resonance (MR) imaging sequences in the brain parenchyma of patients with stroke (1–6). These foci, which are depicted as rounded hypointensities with a diameter smaller than 5 mm, correspond histopathologically to deposits of hemosiderin from previous bleedings (5–7). Due to their small size, these foci are called microbleedings, microhemorrhages (MHs), or lacunar hemorrhages (2). Typically, patients with these lesions do not have symptoms of stroke or any other clinical manifestation at presentation.

The incidence of MHs in healthy volunteers and in patients has been studied (1–3,5,6,8–13), and results indicate that clinically silent MHs (ie, MHs with no detectable signs or symptoms) occur in 3%–6% of healthy elderly subjects (11,13) and 20% of patients with prior ischemic stroke (1,6,9). MHs have been reported as additional findings in 54%–71% of patients with acute spontaneous intracerebral hematoma, with a statistically significant association with arterial hypertension (2,5,6,8,10). A connection between MHs and cerebral microangiopathy has been suggested (8–11). The majority of these studies were retrospective and were performed in Asian populations (1–3,5,6,8,12,13).

The clinical importance and prognostic value of MH is still debated (10). These lesions have been interpreted as markers for vessel wall disorders with a consequent vascular vulnerability that increases the tendency of intraparenchymal bleeding (4). Patients with such lesions may have a higher risk of symptomatic spontaneous hematoma, and contradictory data have been published on the regional association between MHs and spontaneous hemorrhage (10,14); MHs can represent an increased risk for recurrent bleeding after an acute hemorrhagic event (10) or a risk of cerebral bleeding after brain ischemia (1,9,15). Furthermore, patients with ischemic stroke and MHs may have a higher risk of bleeding complications with oral anticoagulation (12) or after thrombolysis, with controversial results in the literature (16,17); because MHs directly indicate blood extravasation, this MR imaging evidence, rather than other clinical or morphologic variables, could serve to identify patients at high risk of hemorrhagic complication (12).

However, these facts have not yet been established. Computed tomography (CT), which is unable to demonstrate MHs, is the imaging modality most widely used for evaluating patients after stroke. Therefore, the incidence of MHs, their correlation with signs of cerebral microangiopathy, and their prognostic implications are difficult to assess in daily practice. Further MR imaging studies in patients with stroke are required for a concrete understanding of the importance of the presence of MH. The purposes of our study were to evaluate prospectively with MR imaging the coexistence of MHs in white patients with acute spontaneous intraparenchymal hemorrhage (IPH) and acute ischemic stroke and to examine the association with imaging findings of microangiopathy and various clinical data.

Materials and Methods

Subjects

Before examinations, informed consents were signed either by the patient or by a relative if the patient's clinical condition was poor. The study was carried out with the approval of the local ethics committee. It included 102 patients who had been admitted to the emergency room with suspicion of acute stroke and had no previous history of head trauma, head surgery, or intracranial hemorrhage. Forty-seven of these patients, examined between January 2000 and May 2003, were consecutive patients who had acute spontaneous IPH at presentation, as indicated by means of CT performed on arrival at the hospital, whose clinical condition was good enough to permit an MR examination, and who were willing to participate in the study. Fifty-five patients with stroke and without evidence of intracranial blood at CT were enrolled in the study between September 2002 and May 2003. From these two groups, 45 matching pairs were found. The final study population consisted of 90 patients: 45 patients with IPH (24 men and 21 women; median age, 65 and 68 years, respectively) and 45 control subjects (26 men and 19 women; median age for both, 67 years). Twelve patients (two with IPH and 10 without IPH) were discharged owing to the lack of an adequate match. All patients were examined with MR imaging an average of 2 days after admittance (median, 1.9 days; range, 0.2–90.0 days).

MR Imaging Technique

The MR imaging examinations were performed at 1.5 T. The imaging protocol included transverse spin-echo (SE) T1-weighted (500/14 [repetition time msec/echo time msec], intermediate- and T2-weighted (2300/16–120), fluid-attenuated inversion-recovery (FLAIR) (10 000/140/2000 [repetition time msec/echo time msec/inversion time msec]), and transverse and coronal gradient-echo T2*-weighted (500/14; flip angle, 30°) sequences. The pixel size was 0.98 × 0.78 mm, and the section thickness was 5 mm for all pulse sequences. The intersection gap was 0.5 mm for SE and gradient-echo and 1.0

Published online
10.1148/radiol.2381040551

Radiology 2006; 238:240–247

Abbreviations:
FLAIR = fluid-attenuated inversion recovery
IPH = intraparenchymal hemorrhage
MH = microhemorrhage
SD = standard deviation
SE = spin echo

Author contributions:
Guarantor of integrity of entire study, R.R.; study concepts, R.R., M.A., A.T.; study design, R.R., M.A., P.S., A.T.; literature research, M.A., R.R.; clinical studies, A.S., A.T.; data acquisition, M.A., R.R., P.S., A.S.; data analysis/interpretation, M.A., R.R., P.S.; statistical analysis, M.A.; manuscript preparation and editing, M.A., R.R.; manuscript definition of intellectual content, M.A., R.R., A.T.; manuscript revision/review, R.R., A.T., M.A., A.S.; manuscript final version approval, all authors

Address correspondence to M.A., Hospital Municipal de Badalona (Resonancia Magnética), Via Augusta 9-13, 08911 Badalona, Barcelona, Spain (e-mail: *malemany@crccorp.es*).

Authors stated no financial relationship to disclose.

mm for FLAIR sequences. Diffusion-weighted images were obtained for 50 patients, including 44 of 45 control subjects (the examination could not be completed in one who complained of shoulder pain) and six patients with acute IPH. Transverse isotropic single-shot diffusion-weighted imaging was performed with an echo-planar FLAIR sequence (10 000/95/2100) that had two *b* values: 0 and 1000 sec/mm^2, with diffusion gradients applied in the x, y, and z directions at $b = 1000$ sec/mm^2. Apparent diffusion coefficient maps were calculated.

Image Analysis

The images were assessed in consensus by a radiologist (M.A.) and a neuroradiologist (R.R.) with 7 and 19 years of experience in brain MR imaging, respectively, and without prior knowledge of clinical or laboratory data. The following abnormalities were recorded: acute hematomas, MHs, hyperintensities on FLAIR images, lacunar infarcts, residuals from old hematomas, and ischemic lesions on diffusion-weighted images. Acute hematomas were grouped as *(a)* lobar, involving the cortex and/or white matter regions in both cerebral hemispheres; *(b)* striate or thalamic; or *(c)* infratentorial, involving the cerebellum or the brain stem. MHs were defined as homogeneous, rounded, and well-demarcated foci of signal intensity loss on T2*-weighted gradient-echo images, smaller than 5 mm in diameter and without surrounding edema (Fig 1). MHs were counted and grouped as lobar, striate or thalamic, or infratentorial (in the same locations as acute hematomas). Care was taken to exclude any calcifications detected with CT.

Without knowledge of the results of T2*-weighted images, readers assessed the presence of MHs on SE, FLAIR, and diffusion-weighted MR images and on CT scans. A dark spot depicted on all diffusion-weighted images ($b = 0$ sec/mm^2; $b = 1000$ sec/mm^2 in x, y, and z directions and trace image) was considered an MH. The number and location of MHs were subsequently correlated with those seen on T2*-weighted MR images.

The presence of hyperintensities in the white matter and/or the deep gray matter (basal ganglia or thalamus) on FLAIR images was noted. The changes were visually graded as described in Table 1. The presence and number of lacunar infarcts were recorded; lacunar infarcts were defined as areas less than 10 mm in diameter, hypointense on T1-weighted SE MR images and hyperintense on T2-weighted SE and FLAIR MR images, and with a center isointense to cerebrospinal fluid with all sequences. Small areas of ischemic parenchymal destruction, smaller than 10 mm and isointense to cerebrospinal fluid, were registered as lacunae. In some instances, it was not possible to differentiate lacunae from local widening of Wirchow-Robin spaces.

The presence of residuals from old hematomas was noted, as was the presence of fresh and old ischemic lesions on diffusion-weighted images. Patients with dark foci in the border of the infarcted area on T2*-weighted gradient-echo MR images were excluded, as it was not possible to differentiate be-

Table 1

Visual Rating Scale of Hyperintensities on FLAIR Images

Location of Hyperintensities	Possible Score		
	Right	Left	Sum
Cerebral white matter*	0–3	0–3	0–6
Periventricular†	0–2 caps, 0–2 bands	0–2 caps, 0–2 bands	0–8
Striate body and thalamic‡	0–2	0–2	0–4
Infratentorial§	· · ·	· · ·	0–2
Maximum sum score	· · ·	· · ·	20

* Score of 0, no abnormalities or hyperintensities < 5 mm in longest diameter; 1, hyperintensities 5–10 mm in longest diameter with a distribution that appears punctate; 2, hyperintensities > 10 mm with patchy or early confluent appearance; and 3, confluent hyperintensities.

† Score of 0, absent or thickness < 5 mm (normal variant); 1, thickness 5–10 mm; and 2, thickness > 10 mm.

‡ Indicates basal ganglia, thalamus, and external and internal capsules. Score of 0, absent; 1, hyperintensities < 5 mm in longest diameter (any number); and 2, hyperintensities > 5 mm in longest diameter (any number).

§ Indicates brainstem and/or cerebellum. Score of 0, no abnormalities; 1, hyperintensities < 5 mm (any location, any number); and 2, hyperintensities > 5 mm (any location, any number).

Figure 1

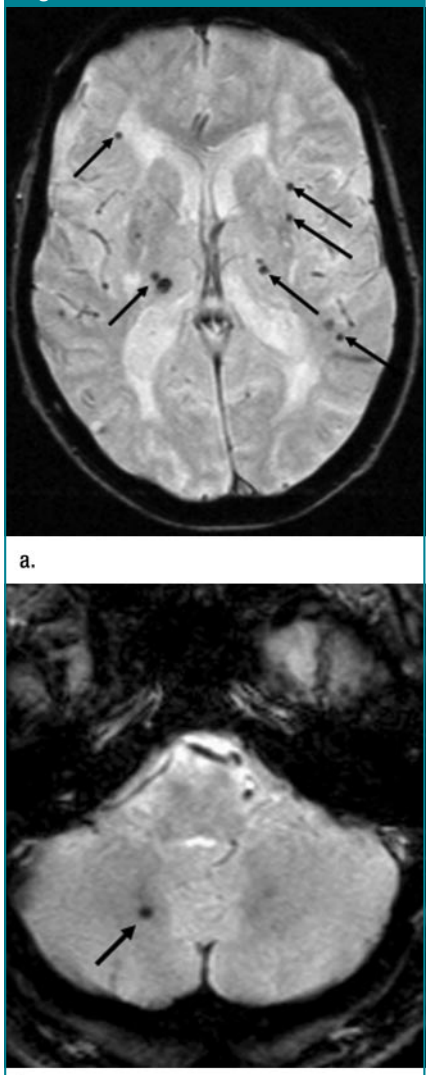

a.

b.

Figure 1: Transverse T2*-weighted gradient-echo images (500/14; flip angle, 30°) show typical MR appearance of MHs **(a)** in a patient with multiple MHs (arrows) and **(b)** in a patient with a single lesion (arrow) in the cerebellum.

tween earlier clinically silent MHs and petechial lesions commonly seen in infarcts as a consequence of ischemic vascular damage. The supratentorial abnormalities mentioned were registered separately for the right and left sides.

Clinical Data

The charts for all patients were reviewed independently by a neurologist (A.S.), and the following data were recorded: *(a)* arterial hypertension, defined as a history of hypertension or repeated blood pressure measurements over 140/90 mm Hg (patients with high blood pressure at arrival at the hospital [or during the first days] that normalized without treatment were not considered to be hypertensive); *(b)* diabetes, defined as either a history of diabetes or a fasting blood glucose level above 6.1 mmol/L (if that level rose during the first few days but normalized without treatment, the patient was not denoted as having diabetes); *(c)* coronary artery disease, defined as a history of myocardial infarction or current treatment for angina pectoris; *(d)* previous stroke, defined as physician-diagnosed symptomatic infarction without evidence of intracranial blood at CT (transient ischemic attacks were not included); *(e)* atrial fibrillation, permanent or paroxysmal, confirmed with electrocardiography; and *(f)* current medical treatment with anticoagulants or antiplatelet agents.

Statistical Analysis

The statistical analysis was done together by our statistical consultant and one of us (M.A.). A statistical software package (STATISTICA 2003, version 6; StatSoft, Uppsala, Sweden) was used for analyses. The relationships between MH and IPH, ischemic lesions, and grades of FLAIR hyperintensities were analyzed by means of regression analysis. The number of MHs was plotted against age to determine whether a relationship between those variables could be established. The relationship between MHs and clinical data were analyzed for patients with IPH and for the control subjects (patients without IPH), also by means of regression analysis. For all tests, P values of less than .05 were considered to indicate a significant difference.

Figure 2

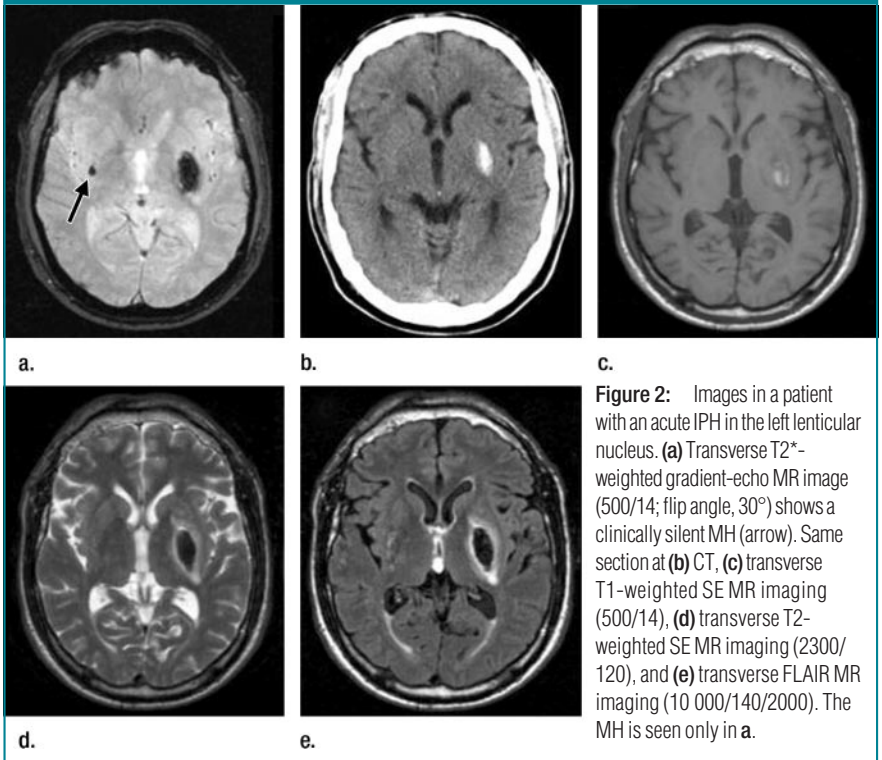

Figure 2: Images in a patient with an acute IPH in the left lenticular nucleus. **(a)** Transverse T2*-weighted gradient-echo MR image (500/14; flip angle, 30°) shows a clinically silent MH (arrow). Same section at **(b)** CT, **(c)** transverse T1-weighted SE MR imaging (500/14), **(d)** transverse T2-weighted SE MR imaging (2300/120), and **(e)** transverse FLAIR MR imaging (10 000/140/2000). The MH is seen only in **a**.

Results

MHs were depicted exclusively on T2*-weighted gradient-echo MR images and were not revealed at CT or at SE and FLAIR MR imaging (Fig 2). MHs were found in 64% of the patients with acute IPH (29 of 45) and in 18% of the control subjects (eight of 45) (patients with stroke without IPH). A significant relationship between MH and IPH was determined ($P < .001$). The mean number of MHs was 3 (median, 1; range, 1–25) in patients with acute IPH, and the mean was 0.5 (median, 0; range, 1–9) in the control group. In the majority of patients, MHs were located in multiple parts of the brain, and most frequently they were striate or thalamic (42%) or lobar (40%). The acute IPH was lobar in 17 of 45 patients (38%), was located in the striate or thalamic region in 21 (47%), and involved the brain stem or cerebellum in seven (16%). In 13 of 45 patients (29%), MHs were detected in the same part of the brain as the acute IPH.

Among the 29 patients with IPH and MH, 83% (24 of 29) had hyperintensities (mean score, 7.3, median, 9; standard deviation [SD], 4.8) and 45% (13 of 29) had lacunae; the corresponding percentages for the 16 patients without MH were 44% (seven of 16) (mean score, 2; median, 0; SD, 3) and 19% (three of 16). Patients with IPH who also had MHs had higher scores for hyperintensities. A relationship between MH and the occurrence and extent of T2 hyperintensities was determined ($P < .001$) (Fig 3). The mean score for hyperintensities for the eight control subjects who also presented with MHs was 7.5 (median, 6.5; SD, 5.6), compared with 3.2 for the 37 control subjects without MHs (median, 0; SD, 5.5). The number of MHs was plotted against age for the patients with and those without acute IPH separately and for all patients together. The scatterplots of the number of MHs revealed no relationship with age (Fig 4).

The distribution of control subjects and patients with IPH, according to the clinical data, is presented in Table 2; the patients in each group are divided into those with and those without MH. Table 2 also presents the median hyperintensity scores and mean ages. No relationship was ascertained between the presence of MH and the clinical data.

The findings at diffusion-weighted MR imaging verified the diagnosis of acute ischemic stroke in 26 of the 44 control subjects (patients without IPH) (60%), of whom 23% (six of 26) showed MHs. Diffusion-weighted MR imaging revealed old infarcts in 13 of the 44 control subjects (30%), one of whom had MHs (8%). The detectability of MHs with diffusion-weighted MR imaging was analyzed in 50 patients. Ten of them had 22 MHs on T2*-weighted MR images. Five of these MHs (23%) were also seen on diffusion-weighted MR images. Diffusion-weighted MR imaging did not depict 77% of MHs (17 of 22) and yielded 24 false-positive findings.

Figure 3

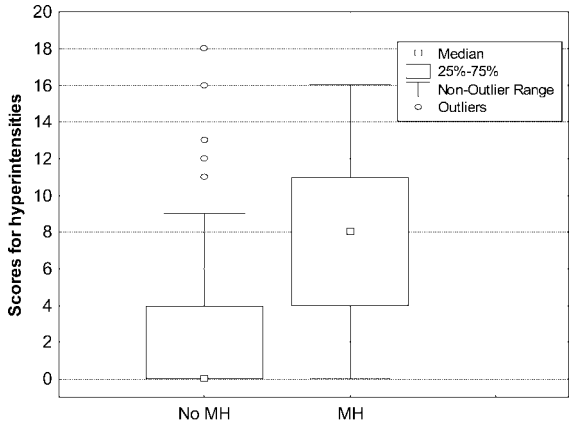

Figure 3: Box plot of distribution of scores for hyperintensities in the white and deep gray matter in patients with acute IPH ($n = 45$). The patients are divided into two groups: those with MH ($n = 29$) and those without ($n = 16$). Scores were higher in patients with MH.

Figure 4

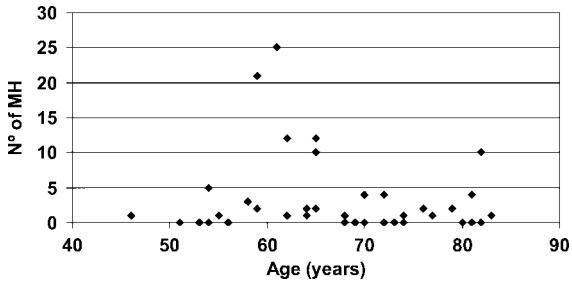

Figure 4: Scatterplot of the number of MHs against age in patients with acute IPH. No relationship was revealed between age and the number of MHs.

Discussion

The results of our study showed that clinically silent MHs were frequent in patients with acute spontaneous IPH. There was an association between MH and the presence of radiologic signs of microangiopathy in the white and deep gray matter. No relationship was found between MH and the clinical data studied in either group. MHs were identified only at T2*-weighted gradient-echo MR imaging and were invisible at SE and FLAIR MR imaging and at CT. Diffusion-weighted MR imaging was not reliable for the diagnosis of MH.

The coexistence of MHs and acute IPH in our study was similar to that identified in other studies (5,10). The distribution of MHs in different parts of the brain was similar to that found by Roob et al (10), who found 39% of MHs in cortical-subcortical regions and 38% in the basal ganglia or thalami (compared with 40% in cortical-subcortical regions and 42% in the basal ganglia or thalami in our study). With respect to regional associations between MH and the site of acute IPH, no specific patterns of MH distribution were identified; these results concurred with those of Roob et al (10).

Our results differed from those of Lee et al (14), who claimed that cerebral microbleeds are regionally associated with intracerebral hemorrhage. In their study, the parenchyma was divided into large regions for analysis, making it easier to find MHs within the same region as the IPH. MHs in patients with IPH are often multiple, which makes it difficult to analyze regional association. In our opinion, only a follow-up study can reveal a regional relationship; when the hematoma spreads over an area after a bleeding event, it is not possible to determine whether there has been an earlier MH in the same location. MHs may be a marker of generalized small-vessel disease that increases the risk of bleeding, but their presence may not predict the specific region of the brain where IPH will occur.

In our study, MHs were detected in 23% of the control subjects in whom acute ischemic changes were demonstrated with diffusion-weighted MR imaging. This result was similar to the results of Nighoghossian et al (9), who found MHs in 20% of patients with ischemic stroke. Further prospective studies are needed to assess whether such lesions are indicative of a higher risk for hemorrhagic transformation.

An association between MH and radiologic signs of cerebral microangiopathy, measured as the grade of leukoaraiosis and number of lacunae, has been reported (8–11). The results presented in our study provide further evidence that MH reflects severe microangiopathy, with vessel wall injury thus increasing the tendency for bleeding. The changes recorded in both white and deep gray matter and the strong correlation ($P < .001$) between hyperintensities, nonlacunar changes, and the presence of MH, raise the question of how

related they are to the risk of hemorrhagic complications.

A strong association between MH and arterial hypertension has previously been reported (5,10,12). The association was not verified in our study, although a large proportion of patients with hypertension was observed among patients also with MHs.

No association was found between MH and the other clinical conditions analyzed (diabetes, previous stroke, coronariopathy, atrial fibrillation, or anticoagulant or antiplatelet therapy). These results differed from previously published results that indicated an association with diabetes (9) but were in concordance with the results of Roob et al (10). However, the data presented here are not extensive and cannot exclude these associations.

MH has been correlated with age (9,12). In our study, regression analyses for the number of MHs versus patient age indicated no correlation between the two factors for the whole age range. MHs have also been associated with microangiopathy due to cerebral amyloid angiopathy, in which fibrinoid necrosis due to progressive deposition of amyloid within the vessel wall is seen (4). The IPHs in cerebral amyloid angiopathy are typically cortical and lobar. Concomitant MR imaging evidence of cortical-subcortical microbleeding (18) supports this diagnosis. The MHs identified in our study had no predilection sites, and cerebral amyloid angiopathy was not suspected in any of the patients.

Other causes of hemorrhages in the brain include cavernomas and petechial lesions secondary to brain contusions or diffuse axonal injury after head trauma. In an MR imaging classification of cavernous malformations (19), type IV lesions are identical to MHs on T2*-weighted gradient-echo MR images, which means that some of the foci of signal intensity loss in our study might have represented cavernomas.

The diagnosis of brain contusion or diffuse axonal injury was highly unprovable in our study, because patients with previous head trauma were excluded. However, in clinical practice, a bleeding episode is difficult to date because some of these events are clinically silent. In some circumstances, such as after head trauma, the distinction between new MHs, indicating diffuse axonal injury, and old petechial lesions is of vital importance. Small hemorrhages may be undetected with SE MR sequences but are easily detected with T2*-weighted gradient-echo MR sequences (20–23). A study in rabbits (22) demonstrated that it is not possible to differentiate between old (6–7 months) and fresh hemorrhages if they are very small. On susceptibility-weighted MR images, the signal intensity patterns for hematoma residues and small acute hematomas are the same (signal intensity loss). The contrast in both cases is based on the same physical mechanism: the shortening of the T2* relaxation time owing to susceptibility effects, caused by hemosiderin and ferritin in chronic hematomas and by deoxyhemoglobin in intact red blood cells in acute hematomas. Similar results were obtained in the present study; some small lesions were detected only on T2*-weighted MR images, and their age could not be determined by means of image characteristics.

T2*-weighted gradient-echo MR sequences are accurate for detecting small amounts of blood products (20,24–26). In our study, MHs were detected only with T2*-weighted gradient-echo MR imaging and were invisible with CT and with SE and FLAIR MR imaging. Epiplanar sequences are intrinsically susceptibility weighted, and diffusion-weighted MR imaging has been recommended for the diagnosis of hemorrhages (26,27); in our study, however, diffusion-weighted MR imaging missed 77% (17 of 22) of MHs depicted with gradient-echo MR sequences. In addition, diffusion-weighted MR imaging resulted in 24 false-positive findings because of the low signal-to-noise ratio of the sequence, which re-

Table 2

Distribution of Patients according to Clinical Data

	Patients with IPH (n = 45)		Control Subjects (n = 45)	
Clinical Data	MH (n = 29)	No MH (n = 16)	MH (n = 8)	No MH (n = 37)
Arterial hypertension				
Yes	23	9	6	21
No	6	7	2	16
Diabetes				
Yes	3	8	1	6
No	26	8	7	31
Clinically diagnosed previous stroke				
Yes	4	0	2	11
No	25	16	6	26
Coronary artery disease				
Yes	3	3	2	9
No	26	13	6	28
Atrial fibrillation				
Yes	1	2	1	7
No	28	14	7	30
Anticoagulant treatment				
Yes	3	0	2	1
No	26	16	6	36
Treatment with antiplatelet agents				
Yes	7	5	2	10
No	22	11	6	27
Median grade of FLAIR hyperintensities	9	0	6.5	0
Mean age (y)	66.2	68.3	69.3	67.1

Note.—Except for the bottom two rows, numbers represent number of patients or control subjects.

sulted in the presence of dark pixels that did not correspond to blood products. In an earlier study (28), 27 of 30 MHs (90%) were missed with use of an SE-based diffusion-weighted MR imaging sequence, but there were no false-positive findings. Results of animal experiments have shown (22) that the areas of susceptibility changes are larger than are residuals of hemorrhages at histopathologic evaluation, and iron deposits in a limited number of cells are disclosed as hypointense foci on MR images. Susceptibility-weighted gradient-echo sequences should be included in MR imaging studies whenever the presence of intracranial blood is suspected, especially if MHs are analyzed.

MHs are better detected at MR imaging with higher field strengths, because susceptibility effects increase to the square of the field strength. High-spatial-resolution MR imaging has improved the detection of qualitative changes of the brain parenchyma, including changes related to microangiopathy (29). Diffuse axonal injury has been more effectively detected with T2*-weighted gradient-echo MR imaging at 3 T than at 1.5 T (30). With the extended clinical use of stronger magnets (eg, 3 T), the detection of MHs and morphologic signs of microangiopathy will improve, thus increasing the understanding of their physiopathologic correlation.

Other causes of signal intensity loss, such as calcium deposits, metallic particles, or air bubbles, can lead to differential diagnostic problems when the brain is imaged with T2*-weighted gradient-echo MR sequences. Signal intensity loss based on vascular flow void at cross sections of blood vessels can give the same MR imaging appearance as small deposits of blood products (hemosiderin). These diagnostic problems can be solved by acquiring MR images in different planes and with the help of other sequences (31) or, occasionally, CT.

The main limitation to this study was the lack of histopathologic confirmation that the so-called MHs actually represented deposits of blood-breakdown products. However, the foci of signal intensity loss in the present study were identical to the MR imaging characteristics that represent deposits of hemosiderin in lesions analyzed histopathologically in both patients (5,7) and animals (20,22); thus, we believe that these foci were signs of earlier hemorrhages.

The exclusion of patients whose clinical condition was too poor for them to undergo MR imaging could have caused bias. Their poor condition might be due to the presence of a bigger IPH, accompanied perhaps by more MHs, which might indicate more severe microangiopathy. This fact could have been detected only with MR imaging.

The clinical implications of diagnosing MH could include the prevention of hemorrhagic complications after thrombolysis. Intravenous and intraarterial thrombolysis improve outcomes when administered to selected patients with acute ischemic stroke. A limitation of these therapies is the occurrence of hemorrhagic transformation, which is symptomatic in 6%–10% of patients (17). Although the risk factors for bleeding during anticoagulation after cerebral ischemia have been studied (32–34), none of the patients evaluated were examined with MR imaging, and MHs were not mentioned as a possible risk factor.

Prior intracerebral hemorrhage is a contraindication to thrombolysis, but there are no guidelines for the treatment of patients with previous asymptomatic hemorrhages, most often MHs, detected only with MR imaging (17). Kidwell et al (17) postulated the need to exclude the presence of MH with brain MR imaging before thrombolysis. Although the majority of cases of hemorrhagic transformation after thrombolytic therapy may be caused by disruption of the blood-brain barrier in acutely injured tissue, some bleeding may be associated with small-vessel injury or MH, particularly those hemorrhages located in regions remote from the acute ischemic field (17).

The effect of MHs on the risk of cerebral bleeding after thrombolysis has been evaluated in a retrospective study (16) analyzing the presence of MHs on pretreatment T2-weighted MR images in 44 patients with acute ischemic stroke. The results suggest that patients with stroke with a small number of MHs can be treated safely with thrombolysis. Larger prospective studies including T2*-weighted MR imaging are needed to address the predictive value of the detection of MHs with regard to the risk of tissue plasminogen activator–induced IPH. The results of further MR imaging investigations could lead to changes in the policy for thrombolytic therapy and to the establishment of new guidelines.

In conclusion, the results from a white population confirm previous results and support the hypothesis of a correlation between the presence of clinically silent MHs, radiologic signs of microangiopathy (T2 hyperintensities and lacunae), and acute IPHs. The detection of MHs is of diagnostic importance and may indicate microangiopathy with an increased risk of bleeding. This raises the question of whether brain MR imaging including susceptibility-weighted gradient-echo sequences should be routinely performed for correct management of patients with stroke, especially before thrombolysis for pretreatment evaluation. Whether patients with MH should be excluded from thrombolytic therapy requires further investigation.

Acknowledgment: We thank Markus Koisti, MS, for his help with the data analysis.

References

1. Fan YH, Zhang L, Lam WW, Mok VC, Wong KS. Cerebral microbleeds as a risk factor for subsequent intracerebral hemorrhages among patients with acute ischemic stroke. Stroke 2003;34:2459–2462.

2. Kinoshita T, Okudera T, Tamura H, Ogawa T, Hatazawa J. Assessment of lacunar hemorrhages associated with hypertensive stroke by echo-planar gradient-echo T2*-weighted MRI. Stroke 2000;31(7):1646–1650.

3. Kwa V, Franke C, Verbeeten B, Stam J. Silent intracerebral microhemorrhages in patients with ischemic stroke. Ann Neurol 1998;44:372–377.

4. Roob G, Fazekas F. Magnetic resonance im-

aging of cerebral microbleeds. Curr Opin Neurol 2000;13:69–73.

5. Tanaka A, Ueno Y, Nakayama Y, Takano K, Takebayashi S. Small chronic hemorrhages and ischemic lesions in association with spontaneous intracerebral hematomas. Stroke 1999;30:1637–1642.

6. Tsushima Y, Tamura T, Unno Y, Kusano S, Endo K. Multifocal low-signal brain lesions on T2*-weighted gradient-echo imaging. Neuroradiology 2000;42:499–504.

7. Fazekas F, Kleinert R, Roob G, et al. Histopathologic analysis of foci of signal loss on GE T2*-w MRI in patients with spontaneous intracerebral hemorrhage: evidence of microangiopathy-related microbleeds. AJNR Am J Neuroradiol 1999;20:637–642.

8. Kato H, Izumiyama M, Izumiyama K, Takahashi A, Itoyama Y. Silent cerebral microbleeds on T2*-weighted MRI: correlation with stroke subtype, stroke recurrence, and leukoaraiosis. Stroke 2002;33:1536–1540.

9. Nighoghossian N, Hermier M, Adeleine P, Blanc-Lassere K, Derex L, Honnorat J. Old microbleeds are a potential risk factor for cerebral bleeding after ischemic stroke: a gradient-echo T2*-weighted brain MR study. Stroke 2002;33:735–742.

10. Roob G, Lechner A, Schmidt R, Flooh E, Hartung H, Fazekas F. Frequency and location of microbleeds in patients with primary intracerebral hemorrhage. Stroke 2000;31:2665–2669.

11. Roob G, Schmidt R, Kapeller P, Lechner A, Hartung H, Fazekas F. MRI evidence of past cerebral microbleeds in a healthy elderly population. Neurology 1999;52:991–994.

12. Tsushima Y, Aoki J, Endo K. Brain microhemorrhages detected on T2*-weighted gradient-echo MR images. AJNR Am J Neuroradiol 2003;24:88–96.

13. Tsushima Y, Tanizaki Y, Aoki J, Endo K. MR detection of microhemorrhages in neurologically healthy adults. Neuroradiology 2002;44:31–36.

14. Lee SH, Bae HJ, Kwon SJ, Kim YH, Yoon BW, Roh JK. Cerebral microbleeds are regionally associated with intracerebral hemorrhage. Neurology 2004;62:72–76.

15. Kim E, Na D, Ryoo JW, Kim SS, Yoon JH. Prediction of hemorrhagic transformation in hyperacute MCA infarction: emphasis on Gd-enhancement, old microbleeds and old hemorrhage on MRI imaging (abstr). In: Radiological Society of North America Scientific Assembly and Annual Meeting Program. Oak Brook, Ill: Radiological Society of North America, 2003; 314.

16. Derex L, Nighoghossian N, Hermier M, et al. Thrombolysis for ischemic stroke in patients with old microbleeds on pretreatment MRI. Cerebrovasc Dis 2004;17(2-3):238–241.

17. Kidwell CS, Saver JL, Villablanca JP, et al. Magnetic resonance imaging detection of microbleeds before thrombolysis: an emerging application. Stroke 2002;33:95–98.

18. Greenberg SM, Finklestein SP, Schaefer PW. Petechial hemorrhages accompanying lobar hemorrhage: detection by gradient-echo MRI. Neurology 1996;46:1751–1754.

19. Zabramski JM, Wascher T, Spetzler R, et al. The natural history of familial cavernous malformations: results of an ongoing study. J Neurosurg 1994;80:422–432.

20. Alemany Ripoll M, Gustafsson O, Siösteen B, Olsson Y, Raininko R. MRI follow-up of small experimental intracranial haemorrhages from hyperacute to subacute phase. Acta Radiol 2002;43(1):2–9.

21. Ripoll MA, Raininko R. Experimental intracerebral and subarachnoid/intraventricular haemorrhages. Acta Radiol 2002;43(5):464–473.

22. Ripoll MA, Siösteen B, Hartman M, Raininko R. MR detectability and appearance of small experimental intracranial hematomas at 1.5 T and 0.5 T: a 6–7-month follow-up study. Acta Radiol 2003;44(2):199–205.

23. Seidenwurm D, Meng TK, Kowalski H, Weinreb JC, Kricheff II. Intracranial hemorrhagic lesions: evaluation with spin-echo and gradient-refocused MR imaging at 0.5 and 1.5 T. Radiology 1989;172:189–194.

24. Gustafsson O, Rossitti S, Ericsson A, Raininko R. MR imaging of experimentally induced intracranial hemorrhage in rabbits during the first 6 hours. Acta Radiol 1999;40:360–368.

25. Patel MR, Edelman RR, Warach S. Detection of hyperacute primary intraparenchymal hemorrhage by magnetic resonance imaging. Stroke 1996;27:2321–2324.

26. Schellinger PD, Jansen O, Fiebach JB, Hacke W, Sartor K. A standardized MRI stroke protocol: comparison with CT in hyperacute intracerebral hemorrhage. Stroke 1999;30:765–768.

27. Ebisu T, Tanaka C, Umeda M, et al. Hemorrhagic and nonhemorrhagic stroke: diagnosis with diffusion-weighted and T2-weighted echo-planar MR imaging. Radiology 1997;203:823–828.

28. Lin DD, Filippi CG, Steever AB, Zimmerman RD. Detection of intracranial hemorrhage: comparison between gradient-echo images and b(0) images obtained from diffusion-weighted echo-planar sequences. AJNR Am J Neuroradiol 2001;22:1275–1281.

29. Hund-Georgiadis M, Ballaschke O, Scheid R, Norris D, von Cramon DY. Characterization of cerebral microangiopathy using 3 Tesla MRI: correlation with neurological impairment and vascular risk factors. J Magn Reson Imaging 2002;15:1–7.

30. Scheid R, Preul C, Gruber O, Wiggins C, von Cramon DY. Diffuse axonal injury associated with chronic traumatic brain injury: evidences from T2*-weighted gradient-echo imaging at 3T. AJNR Am J Neuroradiol 2003;24(6):1049–1056.

31. Gupta RK, Rao SB, Jain R, et al. Differentiation of calcification from chronic hemorrhage with corrected gradient echo phase imaging. J Comput Assist Tomogr 2001;25:698–704.

32. Gorter JW. Major bleeding during anticoagulation after cerebral ischemia. Patterns and risk factors. Neurology 1999;53:1319–1327.

33. Sjöblom L, Hårdemark HG, Lindgren A, et al. Management and prognostic features of intracerebral hemorrhage during anticoagulant therapy: a Swedish multicentric study. Stroke 2001;32:2567–2574.

34. Torn M, Algra A, Rosendaal FR. Oral anticoagulation for cerebral ischemia of arterial origin: high initial bleeding risk. Neurology 2001;57:1993–1999.